X-622-73-160

PREPRINT

66275

THE NIMBUS 4 INFRARED SPECTROSCOPY EXPERIMENT

2. Comparison of Observed and Theoretical Radiances from 425-1450 cm^{-1}

(NASA-TM-X-66275) THE NIMBUS 4 INFRARED SPECTROSCOPY EXPERIMENT. 2: COMPARISON OF OBSERVED AND THEORETICAL RADIANCE FROM 425-1450 cm(MINUS 1) (NASA) ~~36~~ 37 p HC $4.00 CSCL 04A G3/13

N73-27314

Unclas 09186

V. G. KUNDE
B. J. CONRATH
R. A. HANEL
W. C. MAGUIRE
C. PRABHAKARA
V. V. SALOMONSON

JUNE 1973

GSFC

GODDARD SPACE FLIGHT CENTER
GREENBELT, MARYLAND

37

THE NIMBUS 4 INFRARED SPECTROSCOPY EXPERIMENT

2. Comparison of Observed and Theoretical Radiances from 425-1450 cm^{-1}

V. G. Kunde, B. J. Conrath, R. A. Hanel, W. C. Maguire,
C. Prabhakara and V. V. Salomonson

June 1973

Goddard Space Flight Center
Greenbelt, Maryland

THE NIMBUS 4 INFRARED SPECTROSCOPY EXPERIMENT

2. Comparison of Observed and Theoretical Radiances from 425-1450 cm^{-1}

V. G. Kunde, B. J. Conrath, R. A. Hanel, W. C. Maguire,

C. Prabhakara and V. V. Salomonson

ABSTRACT

The Nimbus IV infrared interferometer spectrometer (IRIS) measured the thermal emission of the Earth's atmosphere and surface from 400-1600 cm^{-1} with an apodized spectral resolution of 2.8 cm^{-1}. A comparison of theoretical radiances, computed from in-situ measurements and using a direct integration slant path atmospheric transmittance model, with the observed IRIS radiances has been made to verify the radiometeric and spectral performance of the instrument and to assess the accuracy of the atmospheric transmittances. The radiance comparison has indicated a relatively constant difference of less than 5% in the water vapor continuum in the 425-550 cm^{-1} and 750-1200 cm^{-1} atmospheric "window" regions while in the 667 cm^{-1} CO_2 band the difference was 5-10%. The absolute accuracy was found to be ~ 5-10% for each of the parameters; measured radiances, in-situ measurements, and the atmospheric transmittances, thus it is not possible to uniquely specify the degree of error arising from each parameter in the total resultant difference. Because of the

magnitude of the errors in the measured radiances and in the in-situ measurements and due to the insensitivity of the radiances to the atmospheric transmittances, it is very difficult to improve atmospheric transmittances through the radiance comparison technique.

CONTENTS

THE NIMBUS 4 INFRARED SPECTROSCOPY EXPERIMENT

2. Comparison of Observed and Theoretical

Radiances from 425-1450 cm^{-1}

I. INTRODUCTION

One of the instruments carried on the Nimbus 4 meterological satellite was the infrared interferometer spectrometer (IRIS) which measured the thermal emission of the Earth's atmosphere and surface from 400-1600 cm^{-1} with an apodized spectral resolution of 2.8 cm^{-1}. The instrument and its performance have been described by Hanel et al., 1971, with the instrumental calibration and an overview of the observed spectra presented by Hanel et al., 1972. This paper is the second in a series devoted to the interpretation of the Nimbus 4 IRIS data.

Physical interpretations of the IRIS spectra, to be discussed in subsequent papers, include retrieval of atmospheric temperature, water vapor, and ozone profiles, surface temperature determination, investigation of aerosol effects, and other studies. However, before proceeding with the interpretation of the data, a comparison of measured and computed radiances is made. The models employed in the calculation of the synthetic radiances contain atmospheric transmittances which are also used in the retrieval of atmospheric and surface parameters. The comparison permits an assessment of the consistency of these transmittances with the observed data. A similar investigation was carried out for Nimbus 3 IRIS by Conrath, et al., 1970.

The radiance comparisons are made for selected cases for which near-simultaneous in-situ measurements of atmospheric conditions are available. Although the number of cases studied must necessarily be limited, the results permit significant conclusions to be drawn on the compatibility of the models with the measurements. Emphasis in the comparison is directed toward the water vapor continuum absorption regions at 425-550 and 750-1200 cm^{-1}, and the CO_2 absorption region from 500-800 cm^{-1}.

II. COMPUTATIONAL MODEL

The radiances have been calculated by numerical integration of the radiative transfer equation, assuming local thermodynamic equilibrium. The direct integration slant path transmittance model and radiative transfer solution used are described in detail by Kunde and Maguire (1973). The main improvement in the transmittance model over that employed in the Nimbus 3 investigation (Conrath et al., 1970) is in the water vapor continuum which now employs the two parameter model of Bignell (1970). The water vapor continuum absorption coefficient consists of two components, one proportional to the total pressure ($\propto k_1 P$) and the other to the partial pressure of water vapor ($\propto k_2\ e$). In the 1000 cm^{-1} region the e-type absorption is dominant. As in the earlier work, absorption by the 1285 cm^{-1} N_2O band and the 1306 cm^{-1} CH_4 band was included using a band model representation (Green and Griggs, 1963). The effect of the strong O_3 absorption in the 1000-1100 cm^{-1} region has not been included in the computed spectrum.

The computational model assumes a knowledge of the surface pressure, temperature, and spectral emissivity, along with the atmospheric composition and temperatures. Compositional information includes the amount and distribution of optically active gases such as CO_2, H_2O, O_3, CH_4, and N_2O. The computed monochromatic radiances are convolved with the IRIS instrument function to obtain spectra with a resolution compatible with the measured spectra.

III. IN-SITU MEASUREMENTS

The comparison between the observed and calculated spectra must be carried out for cases with the in-situ and satellite measurements coincident in space and time. It is also desirable to have comparison cases for a range of climatological conditions to verify the dependence of the absorption on the temperature and on the abundance of variable molecular constituents. Of particular interest is the behavior of the water vapor continuum in the more transparent spectral regions.

When attempting to apply this technique of validating observed data and verifying atmospheric transmittances, several problems associated with the in-situ measurements are encountered. First, the satellite instrument measures radiation from a 3-dimensional spatial region of the atmosphere and from the underlying surface while the in-situ measurements yield, at best, only data from the local environment of the sensing element. Thus horizontal homogenity within the field-of-view must be assumed. Second, exact time and space coincidence is not possible as the radiosonde measurements are obtained over an ascent time of 4 to 5 hours while the satellite measurements are nearly instantaneous (~13 secs for IRIS). Third, the in-situ measurements themselves have limited accuracy. Further restrictions on the radiance comparison technique arise from the unknown effects of surface emissivities, clouds and aerosols not included in the computational model. To minimize these effects, clear atmosphere conditions were chosen with an oceanic lower boundary where possible. When all of the above restrictions are taken into consideration, the number of suitable cases is severely limited.

Two ocean areas have been selected for this comparison. One area is in the vicinity of Wallops Island and the other near Guam. In the Wallops area, a concerted large scale effort to obtain in-situ measurements by radiosondes and rocketsondes, coincident with Nimbus 3 and 4 over-flights, was carried out between June 8 and September 23, 1970 (Rocket/Nimbus Sounder Comparison (RNSC), 1972). Thirty-eight sets of coincident measurements were compiled. Temperatures in the 20-60 km altitude range were obtained with two types of rocketsondes, the Arcasonde and the Datasonde. Temperatures measured by the Datasonde are considerably higher than those derived from the Arcasonde. The temperature profiles employed in the present study are a combination of the original rocket and radiosonde data provided by the Upper Air Branch of NOAA. For Guam, the satellite pass occurs at synoptic times and therefore the standard high altitude radiosonde measurements were used in conjunction with a climatological extrapolation for the upper atmosphere.

For this comparison two mid-latitude clear cases have been chosen from the RNSC set. One of these cases occurred over the ocean, on June 25th, while the second, on June 8th, had to be selected over land due to cloud interference over the ocean portion of the orbit. The comparison case for the tropical type atmosphere in the Guam area was on April 27, 1970. The atmospheric temperature profiles for these cases are shown in Figure 1, and several of the salient features are summarized in Table 1. The tropical (Guam) case represents the wettest atmosphere with 3.2 precipitable cm of water vapor while the mid-latitude (Wallops Island) cases contain 1.7 and 2.4 precipitable cm.

The surface temperatures listed in Table 1 were obtained from several sources. The value of 301.2°K for the Guam case was derived from an analysis of ship observations by Fleet Numerical Weather Center, Monterey, California. The June 8th Wallops Island value over land of 300.2°K was obtained by varying the surface temperature until the theoretical and observed spectra were in agreement at 1140 cm^{-1}. Since an independent measurement of the surface temperature does not exist for this case the spectral window regions are only suitable for relative comparisons. The value of 296.2°K for Wallops Island on June 25th was derived from an analysis of ship reports by the U. S. Naval Oceanographic Office, Washington, D. C. There was considerable meandering of the Gulf stream in the region where the spectrum was taken, and this has complicated the task of selecting the ocean surface temperature for the model calculations.

The precision and accuracy of the in-situ measurements is difficult to access and will vary with the type of sensor. Random errors in the radiosonde temperature measurements have been estimated by Lenhard (1970) to be between 0.2 and 0.3 K. The absolute error is much more difficult to establish but will certainly be higher. Absolute errors of 5-10 C have been reported from rocketsonde-radiosonde comparisons (Minzner, 1972) and from intercomparisons of various types of rocketsondes (Rocket/Nimbus Sounder Comparison (RNSC) 1972). The precision of the radiosonde measurement of relative humidity in the lower troposphere has been estimated to be 10-20% (Meteorological Working Group, 1971).

The random error in the ocean surface temperatures may be 1-2 K due to inaccuracies in the ship readings (Saur, 1963; Booth, 1969) and in the interpretation of the measured water temperatures in terms of the temperature of the radiating surface.

IV. SATELLITE MEASUREMENTS

The Nimbus 4 interferometer records one spectrum every 16 seconds while the motion of the satellite is compensated optically by counter-rotation of the field-of-view. Consequently, each spectrum originates from a circular area of approximately 125 km diameter. These areas are centered along the subsatellite track and separated by approximately the field-of-view diameter and are therefore nearly contiguous. The calibration of the interferometer is accomplished by using an on-board blackbody, the controlled temperature of the instrument, and deep space. A residual emissivity effect of the blackbody, imbalance between space and earth port, and the effect of small periodic instrument temperature changes have been removed. The radiometric precision of the instrument is high with the noise equivalent radiance (NER) being ~ 0.5 erg $sec^{-1}\ cm^{-2}\ sr^{-1}/cm^{-1}$ as estimated from the in-flight calibration (Hanel, et al., 1972).

In addition to the radiometric calibration corrections, a wave number correction has been applied. Although small, this correction becomes important for comparison of sharp spectral features. The finite solid angles of the primary and reference interferometers cause a small wave number shift and a distortion of the true wave number scale. This well known effect, caused by the interference of on-axis and off-axis rays (Connes, 1961; Bell, 1972), has been corrected empirically. A numerical fit of a Gaussian function was made to determine the center wave number position ν_m (ν_t) of the strongest CO_2 and H_2O features in a measured (theoretical) spectrum. The difference $\nu_t - \nu_m$, shown as a function of ν_t in Figure 2, with the crosses representing H_2O lines and the circles CO_2 lines, exhibits considerable scatter. The adopted correction is a linear least squares fit to the data. While random inaccuracies in the theoretical line positions may be partially responsible for the large degree of scatter, it does not seem feasible to attribute all of the scatter to this reason. The determined shift of 0.3 cm^{-1} is only 10% of a spectral resolution element and part of the scatter comes from inaccuracies in the determination of these centers of the measured features.

V. COMPARISON OF THEORETICAL AND MEASURED RADIANCE SPECTRA

The theoretical radiance spectrum for Guam, derived from the computational model and in-situ measurements discussed above, is shown in Figure 3 together with the measured spectrum. The overall agreement is good but differences exist. The ground transmittance spectra corresponding to the Guam and to the June 8th Wallops Island cases are given in Figure 4. The τ_2 and τ_1 are the components of water vapor continuum transmittance associated with the water vapor partial pressure and with the total pressure, respectively. The total transmittance, τ_t, includes the absorption of local water vapor lines.

To examine the residual differences between calculated and observed spectra, the fractional difference between the calculated radiance (N_t) and measured radiance (N_m) is displayed as a function of wave number in Figures 5, 6 and 7. The very ragged appearance of the difference spectra, especially noticeable in the water vapor lines in the 425-550 cm^{-1} and 1225-1450 cm^{-1} regions results mainly from the inadequacy of the wave number transfer function of Figure 2. As a result corresponding molecular lines in the theoretical and observed spectra do not come into exact coincidence giving imperfect cancellation in the difference spectrum. Ignoring the fine structure, the general level resulting from the water vapor continuum is indicated by the broad solid line. The difference spectra will now be considered by spectral region.

A. 425-550 cm^{-1} Region

Absorption in this region of the spectrum is dominated by the pure rotational lines of atmospheric water vapor. The radiometric agreement for the three cases is within 5% in the continuum, this is considerably better than the Nimbus 3 IRIS results where the theoretical water vapor continuum was computed using the concept of a single parameter effective pressure continuum absorption coefficient (Conrath, et al., 1970). This improvement substantiates the validity of the present transmittance model which includes the effect of the e-type H_2O absorption. The radiometric agreement at the line centers is comparable to that of the continuum in the two Wallops Island cases. However for the Guam case the theoretical radiances are underestimated by as much as 10% in the line centers compared to less than 5% in the continuum.

B. 550-750 cm^{-1} Region

The major absorber is the 667 cm^{-1} CO_2 band complex although the 589 cm^{-1} band of N_2O and the 701 cm^{-1} band of O_3 also occur in this region. Neither band has been included in the radiance calculations. The Q branch of the N_2O band absorbs significantly and its presence in the observed spectrum is evident by the $\sim$15% spike at 589 cm^{-1}, the theoretical spectrum being too transparent at this wave number. The 701 cm^{-1} O_3 band absorbs only weakly, yet it is of significance because of its impact on atmospheric temperature retrievals. Total atmospheric transmittance by this band has been computed for the Guam case assuming a .36 cm- atm total ozone content. The resulting atmospheric transmittance at ground level with a 2.8 cm^{-1} resolution is shown in Figure 8. The maximum absorption is ~ 9% in the P and R branch peaks at 686 and 714 cm^{-1} respectively. Inclusion of this absorption in the Guam calculation reduced the fractional radiance difference from ~ .08 to ~ .05 in the O_3 R-branch region, 700-760 cm^{-1}. The effect of the P-branch absorption is minimal as this region is dominated by the strong Q-branch absorption of the 667 cm^{-1} CO_2 band. Although the ozone absorption has only a small effect on the emergent radiance it still must be considered for the temperature inversion problem which is more sensitive to small transmittance errors.

In the 667 cm^{-1} CO_2 band a systematic disagreement in the region of the band center shows theoretical radiances higher than those observed, with maximum differences of ~ 10% for Guam, ~ 10% for June 8, Wallops Island, and ~ 15% for June 25, Wallops Island. The relative difference between June 8 and June 25 is explainable in terms of the systematic differences in stratospheric temperatures measured by the Arcasonde and Datasonde with the Arcasonde considered to be the more accurate system. The disagreement is largest between 625 and 725 cm^{-1}, where the radiation originates from the upper tropopause and lower stratosphere, and is less severe towards both band wings where the radiation originates mostly at the surface and lower tropopause. The vertical region of formation for several selected wave numbers are noted in Figure 1. The largest discrepancies in this region of the spectrum are associated mainly with the lower stratosphere and the upper troposphere. Sources of these discrepancies will be considered further in Section VI.

C. 750-1200 cm^{-1} Region

Molecular absorption arises from the water vapor continuum, with smaller contributions from CO_2, weak water vapor lines, a weak N_2O band at 1167 cm^{-1} and the 1042 cm^{-1} O_3 band. Absorption by ozone in the 1000-1100 cm^{-1} region was not included in the model used in this investigation.

The accuracy of the transmittance function in the "window" portion of the spectrum is of prime interest for the retrieval of surface temperature, for searching for aerosol effects and for investigating surface reststrahlen phenomena. Success in these areas requires accurate knowledge of the water vapor continuum. The spectra of Figures 5-7 shows a relatively constant difference of 5% or less through the 750-950 cm^{-1} regions. The larger deviation in the 1125-1200 cm^{-1} region is accounted for, at least in part, by the absence of the 1167 cm^{-1} N_2O band in the theoretical spectrum. The maximum slant path absorption of this band is 10% and should be taken into consideration in searching for effects of atmospheric aerosols or surface reststrahlen features. The ~5% error in these windows could equally well be in the empirical H_2O continuum absorption coefficients, the ground truth surface temperature as discussed in Section III, or the instrument calibration. The three cases ranging in total H_2O content from 1.7 to 3.2 pr. cm provide a test of the two-parameter H_2O continuum transmittances.

The relatively constant error was obtained with the Bignell k_1 total pressure component taken as approximately zero in the 1000 cm^{-1} region. It was found that use of the upper limit of k_1 measured by Burch (1970) introduced a slope into the difference spectrum. The IRIS spectra thus verify the value of $k_1 \sim 0$ at 1000 cm^{-1} as indicated in earlier work (Wark, 1972; Houghton and Lee, 1972).

D. 1200-1450 cm^{-1} Region

The H_2O band at 1595 cm^{-1}, the N_2O band at 1285 cm^{-1} and the CH_4 band at 1306 cm^{-1} cause absorption in this region. The 10-15% error in the 1250-1400 cm^{-1} region is probably associated with deficiencies in the band models used for the CH_4 and N_2O bands. Further research in this region, using direct integration techniques for CH_4 and N_2O, is currently being pursued.

VI. SOURCES OF ERROR

The radiance comparisons of the previous section have shown generally good agreement between the computations and observations. The major exceptions are the systematic ~5-10% differences in the 625-750 cm^{-1} region and the errors of similar magnitude near 1400 cm^{-1}. The major concern is the large difference in the 667 cm^{-1} CO_2 band where 5-10% is not an acceptable error. To understand this difference it is necessary to attempt to evaluate the magnitude of the error from each of the possible sources: 1) theoretical atmospheric transmittances, 2) in-situ measurements, and 3) absolute instrumental calibration.

The errors in the CO_2 atmospheric transmittances have been estimated as 5-10% (Kunde and Maguire, 1973). This magnitude would only change the calculated radiances by $\sim 1\%$ as they are not very sensitive to the atmospheric transmittance. Also, in the region of greatest disagreement, the maximum contribution to the outgoing radiance comes from the lower stratosphere and upper troposphere where the small temperature lapse rate causes the calculated radiances to be very insensitive to the transmittances. Therefore, it is felt that transmittance errors cannot make a major contribution to the observed discrepancies.

The second potential source of errors is the in-situ measurements. From the Rocket/Nimbus Sounder Comparison (RNSC) study and from discussion of Section III it is apparent that errors of 5-10% are quite possible.

Systematic effects in the instrumental calibration have been examined previously (Hanel, et al., 1972) and correction factors have been developed for their removal. However, it is possible that some residual effects are still present in the calibrated spectra. To obtain a quantitative estimate of the absolute accuracy of the measured radiances IRIS and SIRS B measurements have been compared for eight Wallops Island cases obtained during the RNSC experiment in the June-July 1970 period. Clear atmosphere conditions were chosen to minimize any possible effects due to the different fields-of-view for IRIS (5°) and SIRS (12°). The IRIS radiance corresponding to a SIRS channel was obtained by degrading the IRIS spectrum with the appropriate SIRS spectral response (The Nimbus IV Users Guide, 1970). The average brightness temperature for the eight cases is given for IRIS and for eleven of the SIRS channels in Figure 9 with the corresponding standard deviation shown in Figure 10. The small standard deviation of ~ 1 K in the 600-750 cm^{-1} region denotes a fairly stable atmosphere while the larger values of ~ 2 K in the 800-1250 cm^{-1} region reflect varying surface temperatures. The greater variability in the 425-550 cm^{-1} and 1300-1450 cm^{-1} regions indicate a changing atmospheric water vapor content. The SIRS channels, with the exception of those at 531.5 and 692.0 cm^{-1} indicate about the same standard deviation as IRIS. The 531.5 and 692.0 cm^{-1} channels behave in an anomalous fashion due to instrumental problems (Wark, 1973).

The average difference, SIRS-IRIS, in terms of brightness temperature (ΔT_{bb}), is given in Figure 11 with error bars indicating one standard deviation. The largest and most significant systematic differences are in the 667 cm^{-1} CO_2 band with a maximum of 4 K ($\sim$4erg sec^{-1} cm^{-2} sr^{-1}/cm^{-1}) for the 668.7 cm^{-1} channel decreasing to 1 K for the 750.0 cm^{-1} channel. The differences in the remaining channels lie fairly close to the instrumental NER's with only small systematic differences indicated.

The standard deviation of the in-situ temperature measurements has been computed for the eight cases as a function of height (Figure 12). The spread of 2-4 K over the 0-50 km range, when compared to the ~ 1 K brightness temperature standard deviation for SIRS and IRIS in the 600-750 cm^{-1} region, implies a lower precision in the in-situ measurements than in the satellite measurements. Therefore, improved calibration of remote sensing devices by comparison to in-situ data requires more accurate measurements by the latter technique.

The systematic radiance differences between IRIS and SIRS discussed above and the systematic differences between in-situ temperatures and satellite-inferred temperatures (RNSC, 1971) indicate the absolute calibration as well as the in-situ temperature measurements are largely responsible for the discrepancy noted in the 600-750 cm^{-1} region. These systematic errors must be reduced in magnitude before an attempt can be made to correct CO_2 transmittances by this method.

With the existing imprecise knowledge of the error sources alteration of the calibration or the transmittance model is not justified. However, for applications of the data, it is still necessary to normalize the results for uniformity. In the subsequent Nimbus IRIS application papers such a normalization will be applied.

VII. CONCLUSIONS

The comparison of theoretical and observed radiances indicates a relatively constant error of $\sim 5\%$ in the 425-550 cm^{-1} and 800-1200 cm^{-1} – atmospheric window regions. This good agreement for total water vapor contents ranging from 1.7 to 3.2 pr. cm substantiates the validity of the two parameter approximation of the water vapor continuum, including e-type absorption, in the free atmosphere. The agreement gives confidence in using the IRIS spectra and atmospheric transmittance model for investigating physical phenomena in the window regions, such as determination of surface temperature, aerosol effects, etc. Furthermore, the comparison in the 800-1200 cm^{-1} region indicates that the k_1 component of the water vapor continuum absorption coefficient is essentially zero at 1000 cm^{-1}. Absorption by N_2O bands centered at 589 and 1167 cm^{-1} must be included in quantitative models used in these spectral regions. Absorption by the 1285 cm^{-1} N_2O and 1306 cm^{-1} CH_4 bands must be calculated more precisely than the band model representation used in this study before attempting to extract information on atmospheric N_2O and CH_4 from the 1200-1400 cm^{-1} region of the spectrum.

The radiance comparisons in this paper are based on a set of data from well-calibrated instruments, a set of well-defined specially processed in-situ measurements, and the state-of-the-art atmospheric transmittance model. Yet even under these favorable conditions systematic radiance errors up to 10% in the 667 cm^{-1} CO_2 region are indicated. Systematic differences exist in the absolute calibration, as well as in the in-situ measurements, but is not possible to specify quantitatively the individual error sources. To eliminate or reduce these systematic errors, improvements are needed in the absolute calibration of the remote sensing devices as well as in the calibration of the in-situ instrumentation. More large scale intercomparison experiments, such as the Rocket/ Nimbus Sounder Comparison (RNSC) are needed to assist in the development of absolute calibration techniques. Until such advances can be made, it will be necessary to renormalize measured radiances and/or transmittance models in order to obtain agreement between satellite retrieved temperature profiles and in-situ measurements.

Comparisons of the type described in this paper do not provide an effective means of improving atmospheric transmittance models. While the thermal emission is sensitive to atmospheric temperature through the Planck function, it is relatively insensitive to transmittances. Therefore, with the existing uncertaintities in the in-situ measurements and absolute calibration of the measured radiances, further improvements in transmittances can mainly be expected to come from laboratory measurements or from measurements of atmospheric transmission rather than emission.

ACKNOWLEDGEMENTS

The authors would like to thank G. N. Wolford, H. W. Powell, and F. Rockwell for their computer programming contributions and H. Fleming, NOAA for his assistance in obtaining SIRS B calibrated radiances. The correction to the observed wave number scale is due to L. Herath.

REFERENCES

Bell, R. J., Introductory Fourier Transform Spectroscopy, Academic Press, 382 pp., 1972.

Bignell, K. J., The water-vapor infra-red continuum, Q.J.R.M.S., 96, 390, 1970.

Booth, J. D., Sea-surface temperature patterns in the northeast atlantic, WMO Technical Note No. 103, 77, 1969.

Burch, D. E., Aeronutronic Division Publication U-4784, Philco-Ford Corporation, 31 January, 1970.

Connes, J., Thesis, 1961.

Conrath, B. J., R. A. Hanel, V. G. Kunde, and C. Prabhakara, The infrared interferometer experiment on Nimbus 3, JGR, 75, 5831, 1970.

Green, A.E. S., and M. Griggs, Infrared transmission through the atmosphere, Appl. Opt., 2, 561, 1963.

Hanel, R. A., B. Schlachman, D. Rogers and D. Vanous, Nimbus 4 Michelson interferometer, Appl. Opt., 10, 1376, 1971.

Hanel, R. A., B. J. Conrath, V. G. Kunde, C. Prabhakara, I. Revah, V. V. Salomonson and G. Wolford, The Nimbus 4 infrared spectroscopy experiment 1. Calibrated thermal emission spectra, JGR, 77, 2629, 1972.

Houghton, J. J., and A. C. L. Lee, Atmospheric transmission in the 10-12μm window, Nature, 238, 117, 1972.

Kunde, V. G., and W. C. Maguire, Direct integration atmospheric slant path transmittance model for interpretation of high spectral resolution planetary thermal emission spectra, Submitted to J. Quant. Spectr. & Rad. Transf., 1973.

Lenhard, R. W., Accuracy of radiosonde temperature and pressure-height determination, Bulletin of the American Meteor. Soc., 51, 842, 1970.

Meteorological Working Group, Reliability of meteorological data, Document 110-71, Secretariat, Range Commanders Council, White Sands Missile Range, New Mexico, 1971.

Minzner, R. A., private communication, 1972.

Rocket/Nimbus Sounder Comparison (RNSC), NASA SP-296, 1972.

Saur, J.F.T., A Study of the quality of sea water temperatures reported in logs of ships weather observations, J. Appl. Met., 2, 417, 1963.

The Nimbus IV Users Guide, Nimbus Project Office, Goddard Space Flight Center, Greenbelt, Md., March, 1970.

Wark, D. Q., Atmospheric transmittances used in indirect soundings of the earth's atmosphere, Proceedings of the International Radiation Symposium, Sendai, Japan, May 26-June 2, 1972, p. 554.

Wark, D. Q., private communication, 1973.

Table 1
Summary of Comparison Cases

Location	Latitude	Longitude	Date	Satellite Time	Rocket-sonde	U_{H_2O} (pr cm)	T (K)	Observed Temperature at 899 cm^{-1} (K)
Guam	15.1 N	215.3 W	4/27/70	2 hr 2 min 31 sec		3.16	301.2	296.1
Wallops Is.	37.7 N	76.9 W	6/8/70	16 hr 28 min 23 sec	Arcasonde	1.69	300.2	296.2
Wallops Is.	38.9 N	69.9 W	6/25/70	15 hr 58 min 31 sec	Datasonde	2.43	296.2	292.2

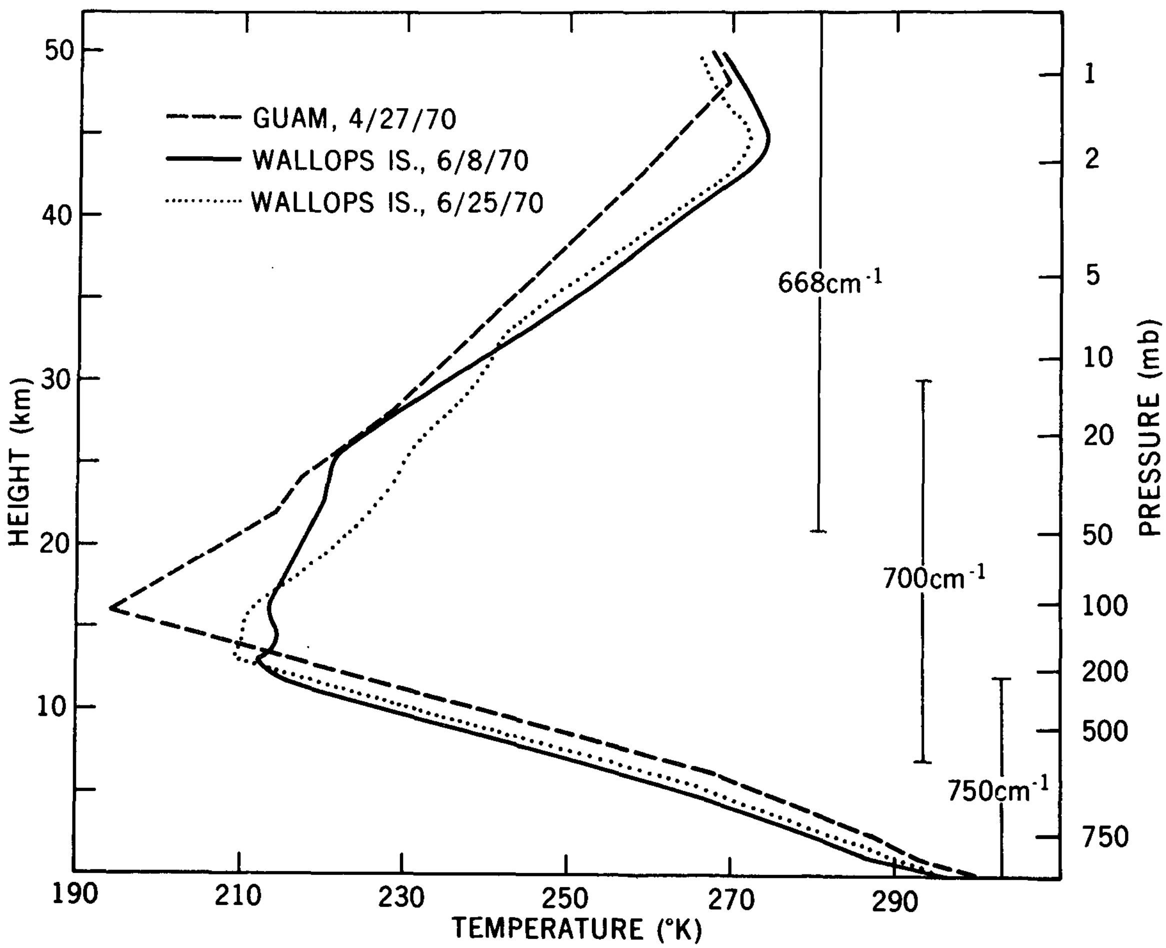

Figure 1. Vertical temperature profiles for radiance comparison atmospheres. The approximate regions of formation for 668, 700 and 750 cm^{-1} are indicated.

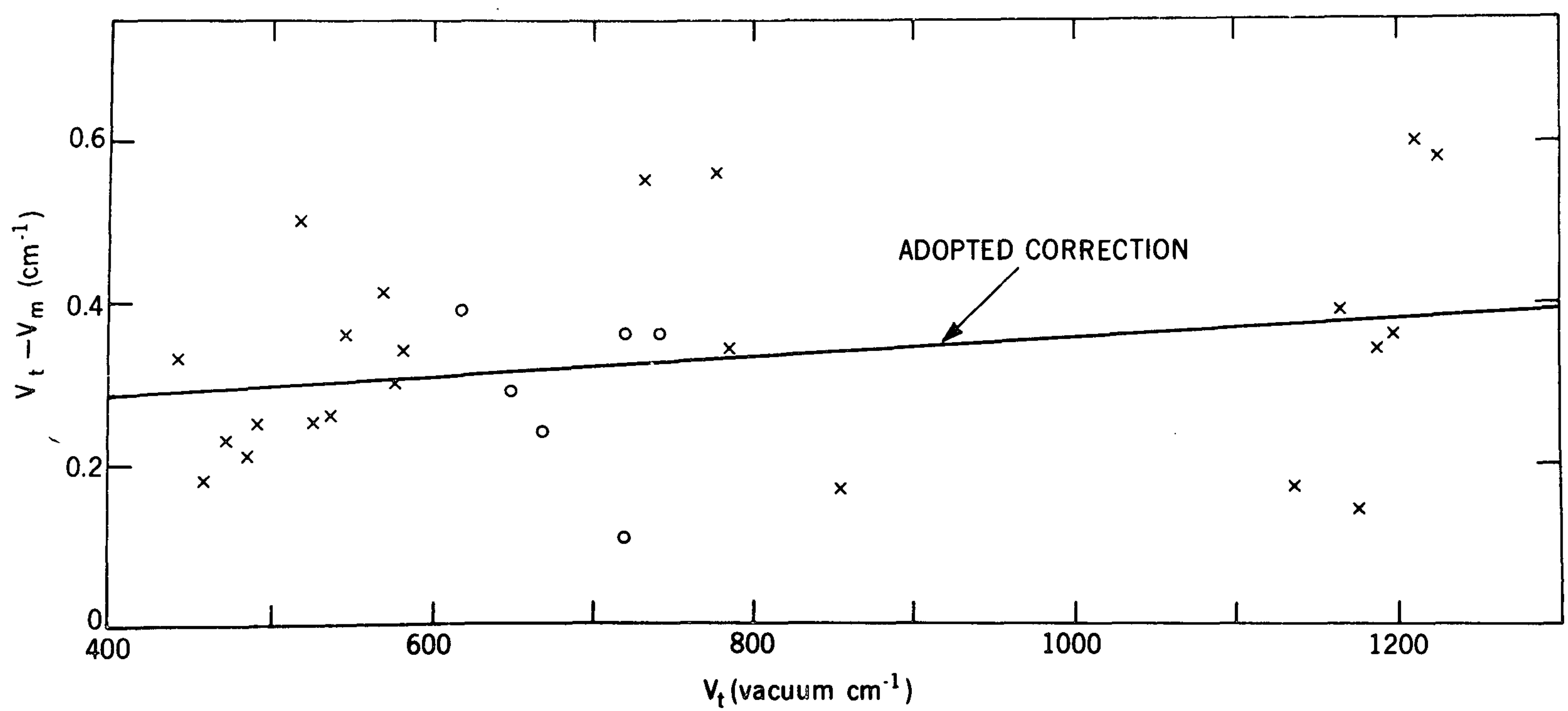

Figure 2. Wave number transfer function to correct observed wave number for finite field-of-view effects.

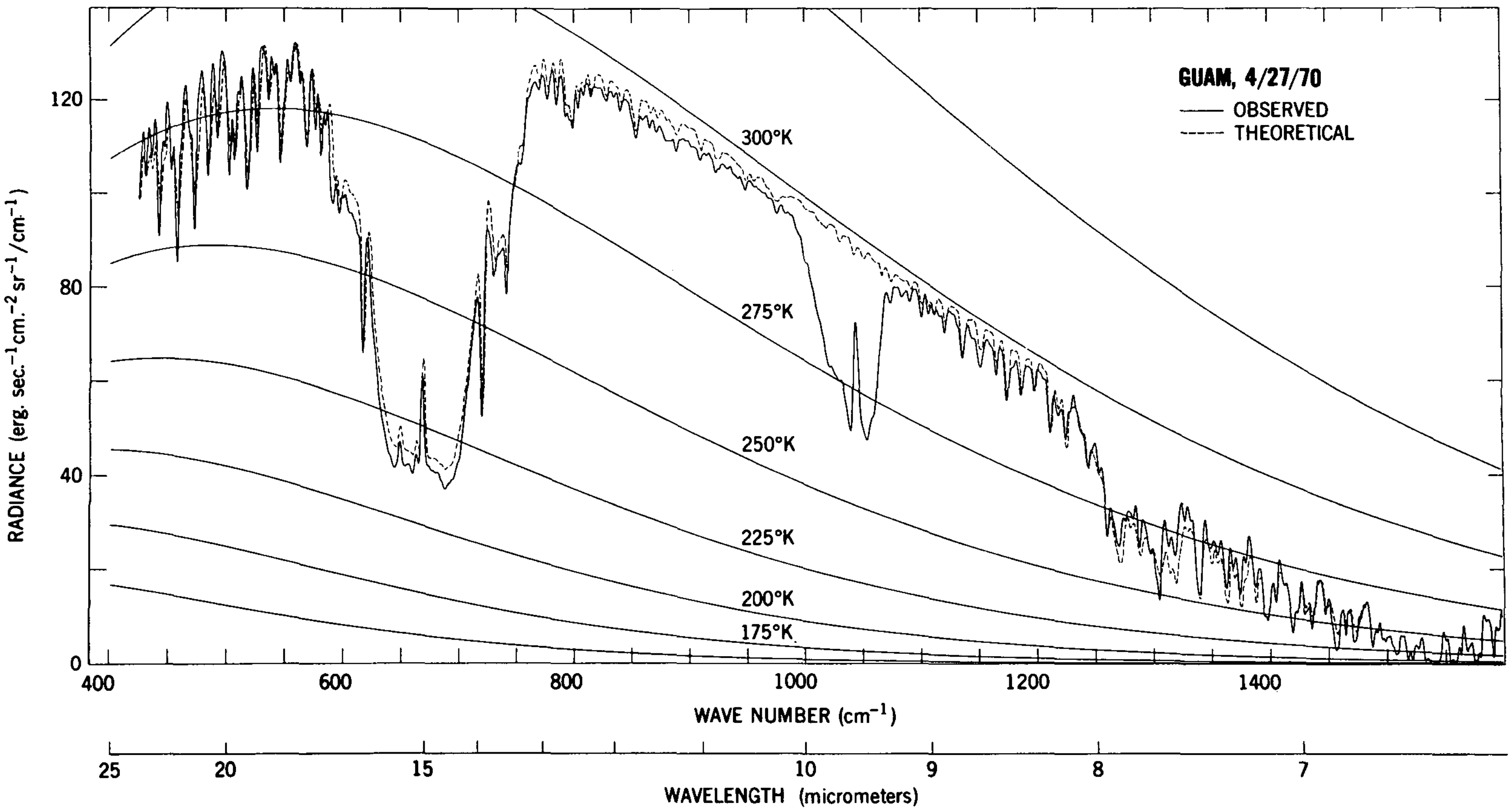

Figure 3. Comparison of observed and theoretical radiances for a clear atmosphere near Guam at 15.1° N latitude and 215.3° W longitude on April 27, 1970.

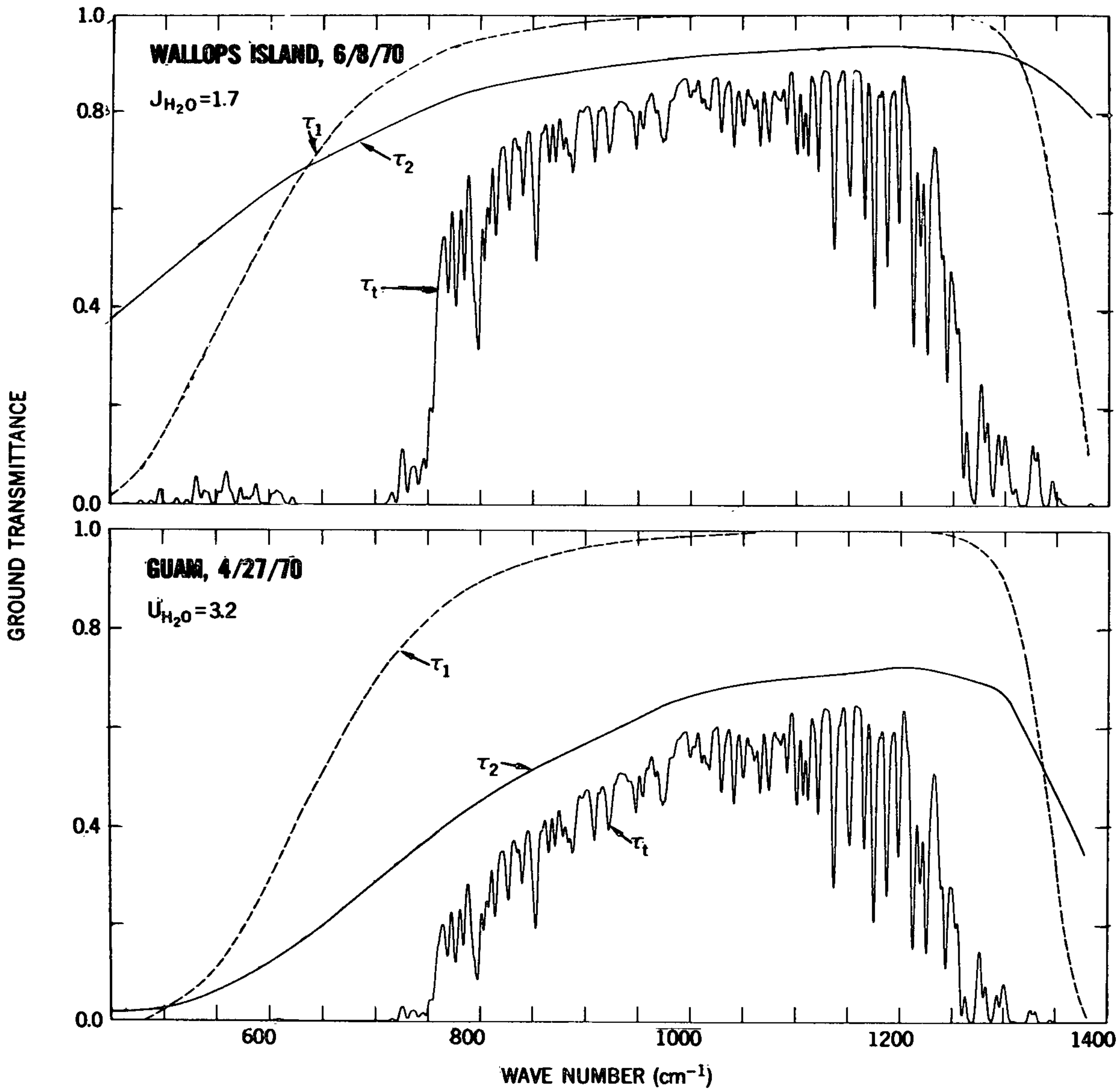

Figure 4. Transmittance from the ground to the top of the atmosphere.

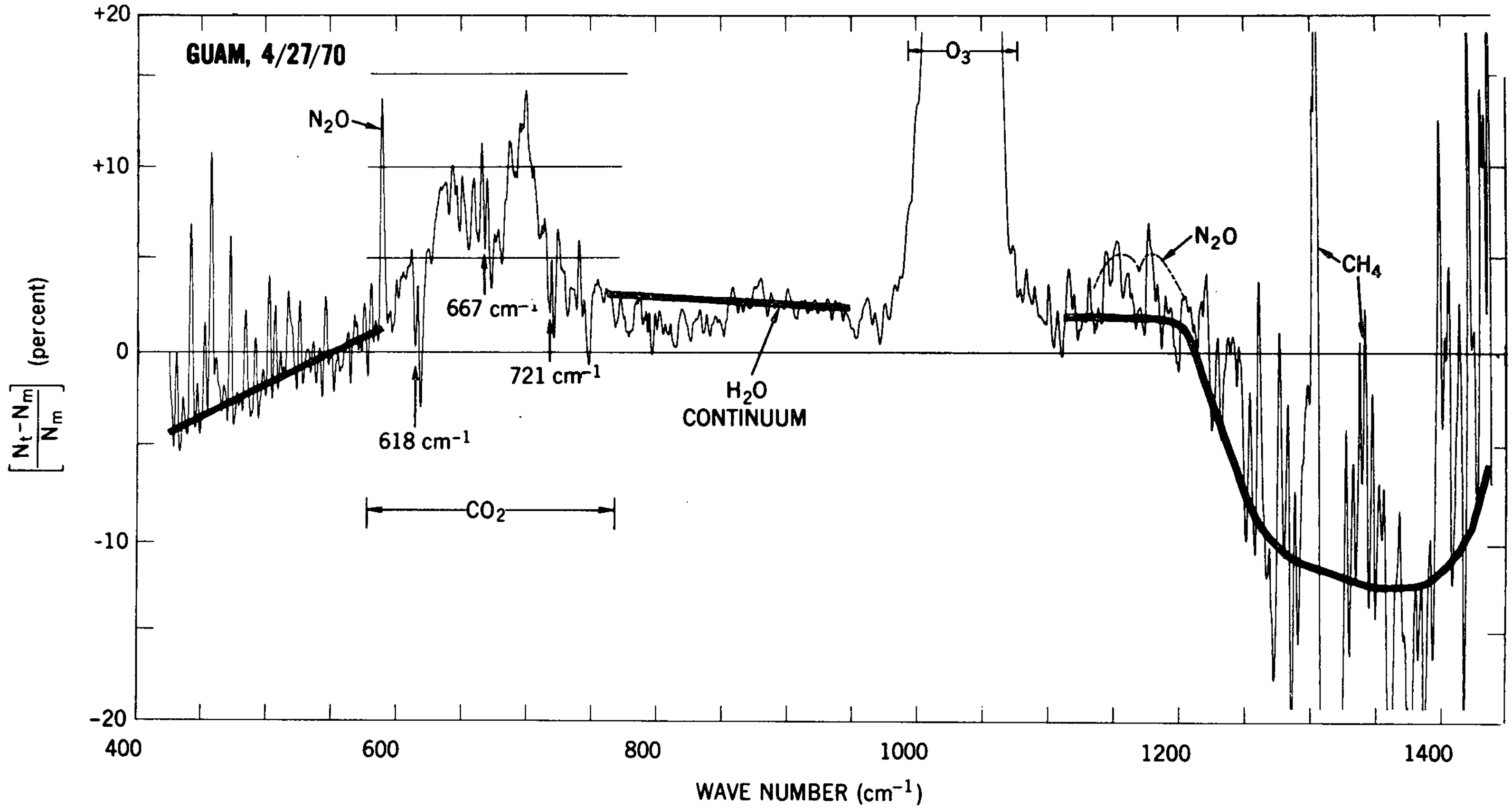

Figure 5. Radiance difference spectrum for the Guam case.

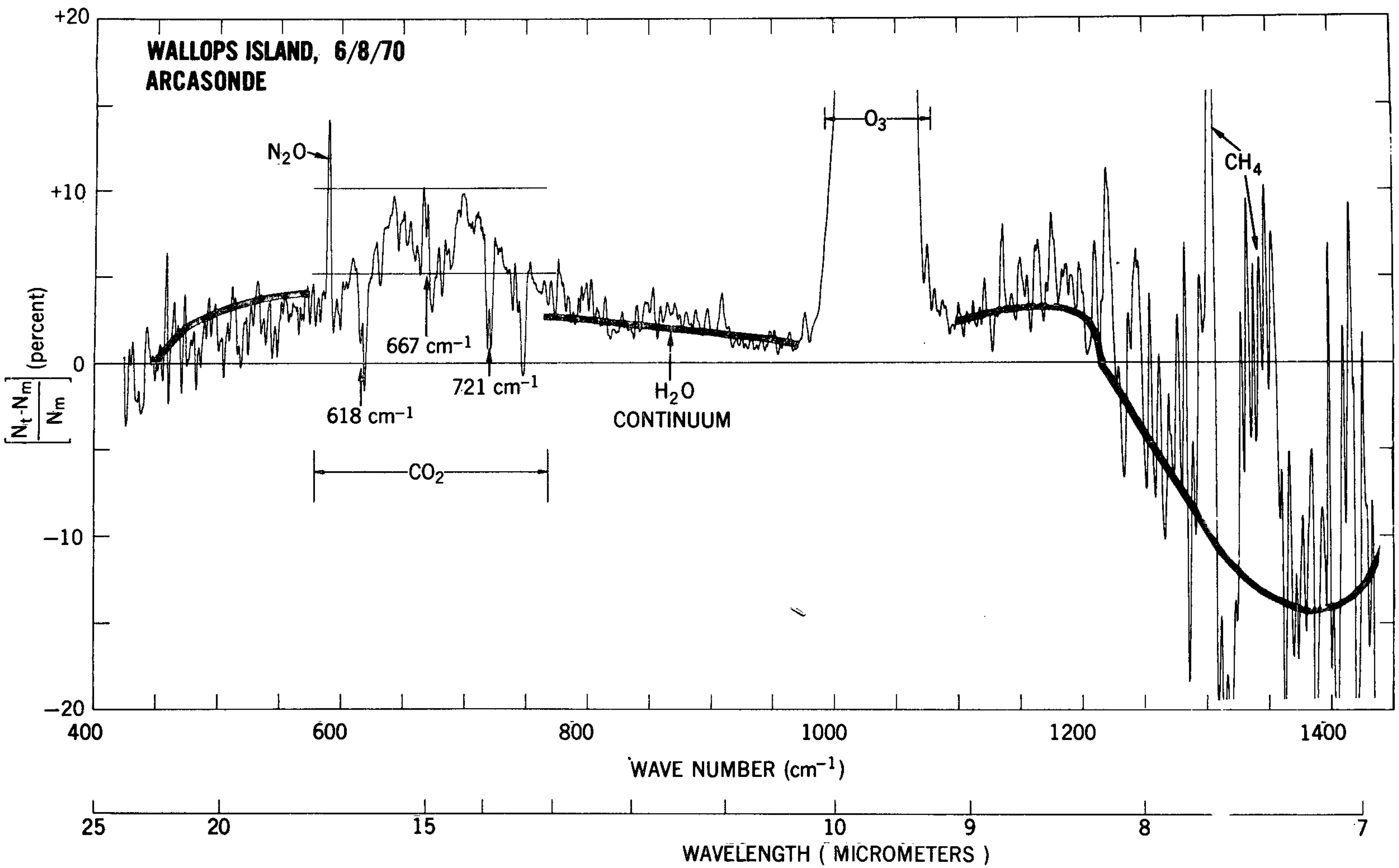

Figure 6. Radiance difference spectrum for June 8, 1970, Wallops Island case.

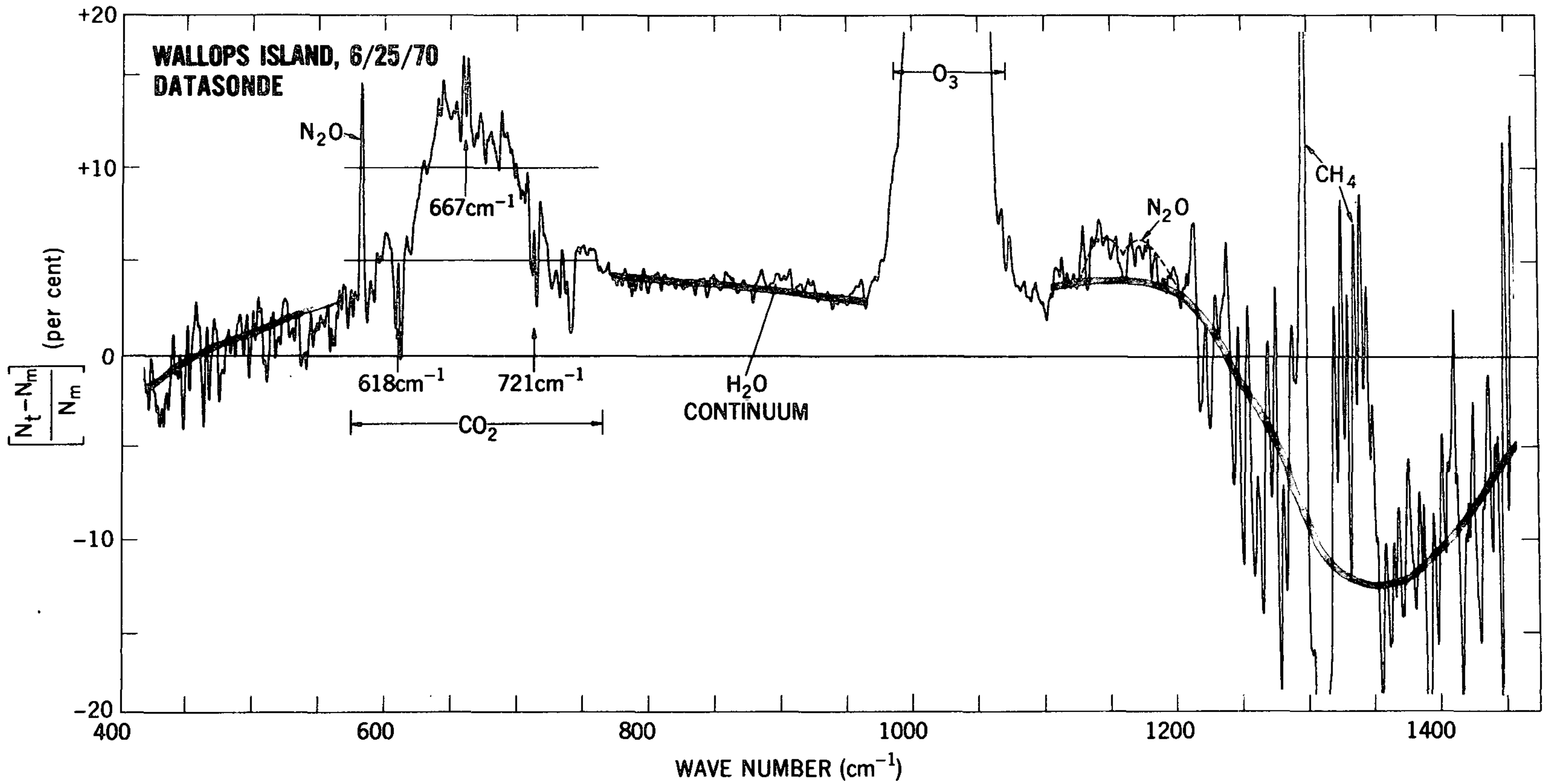

Figure 7. Radiance difference spectrum for June 25, 1970, Wallops Island case.

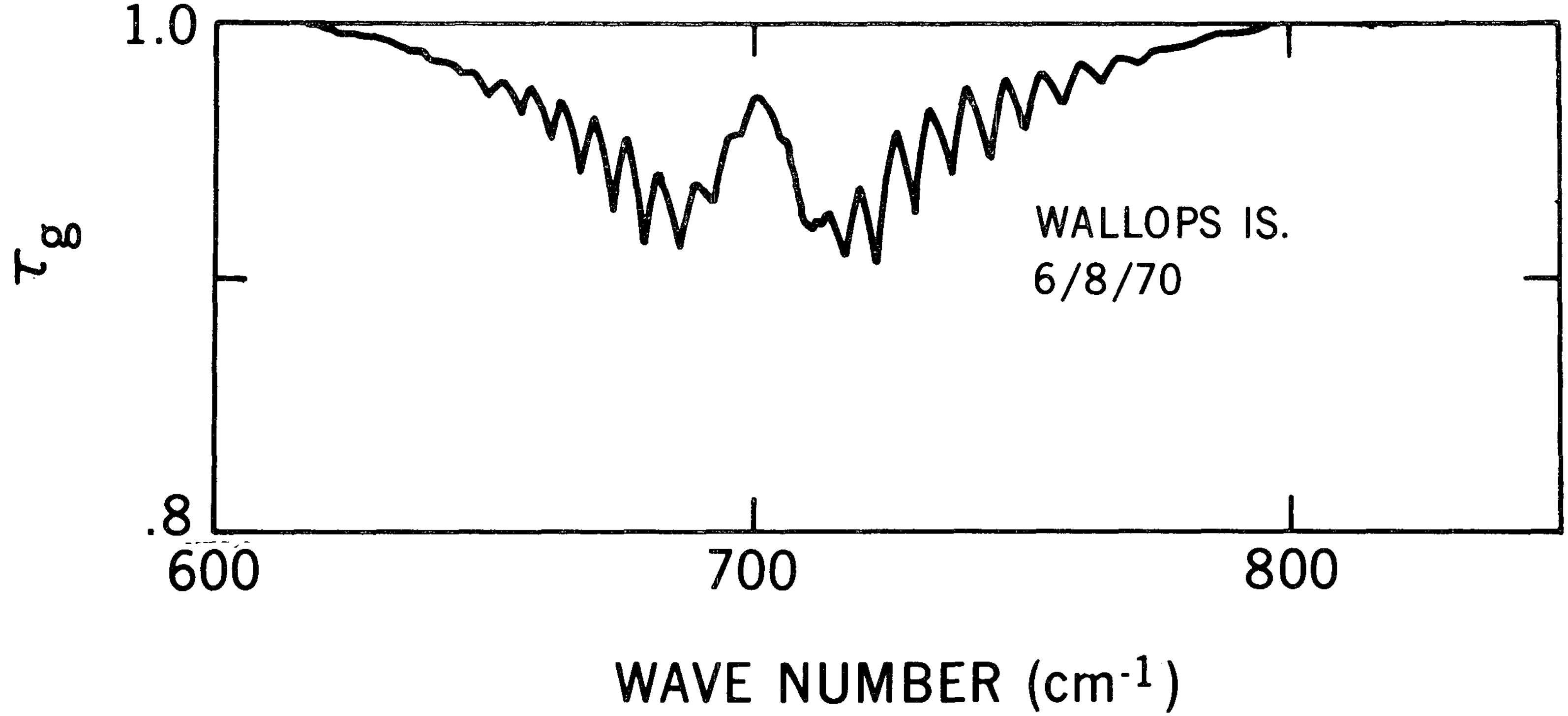

Figure 8. Transmittance from the ground to the top of the atmosphere for a total ozone depth of .36 cm. atm. The spectral resolution is 2.8 cm^{-1}.

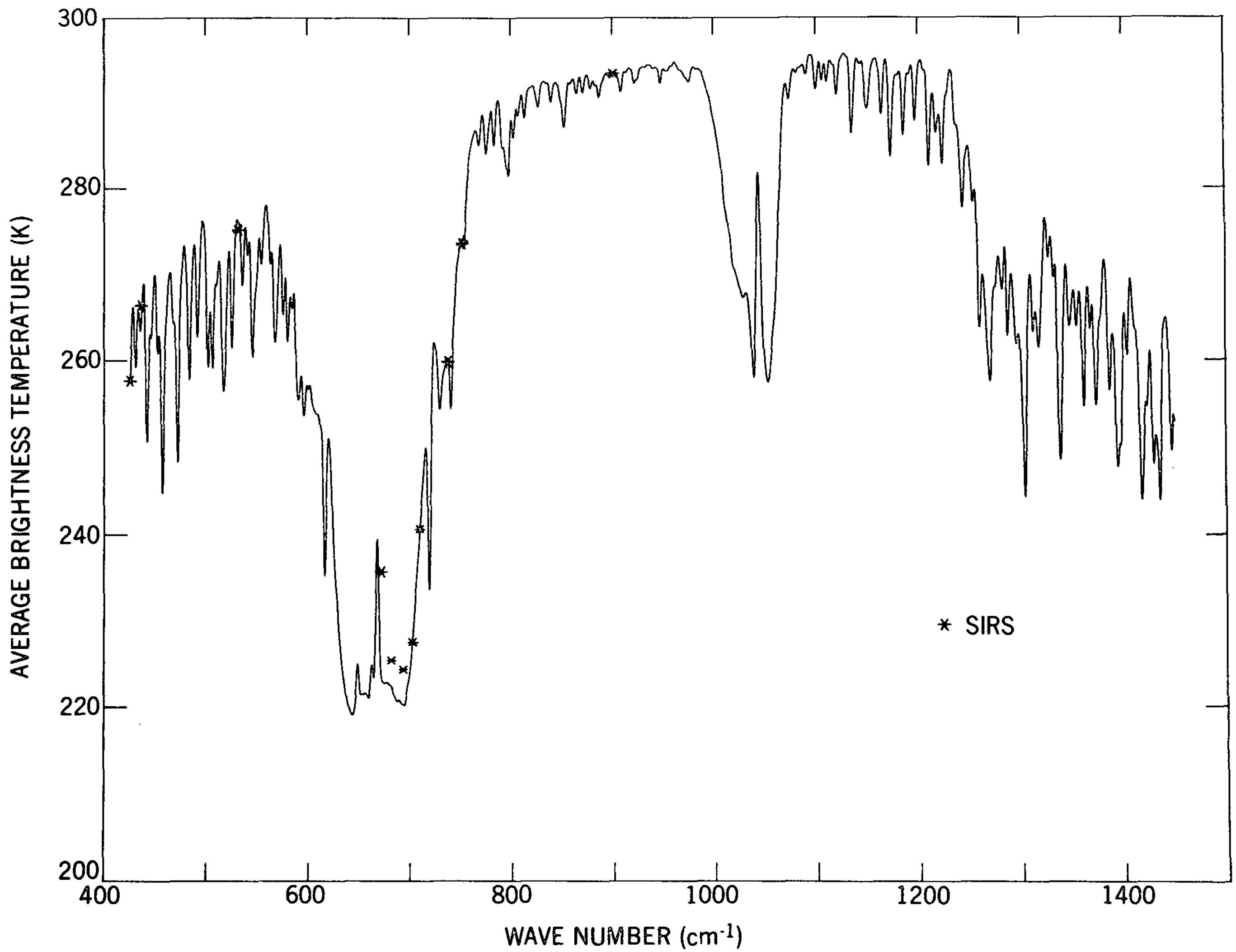

Figure 9. Average brightness temperatures for eight clear atmosphere cases over the Atlantic Ocean near Wallops Island in June - July, 1970. SIRS B measurements obtained at the same time are also included.

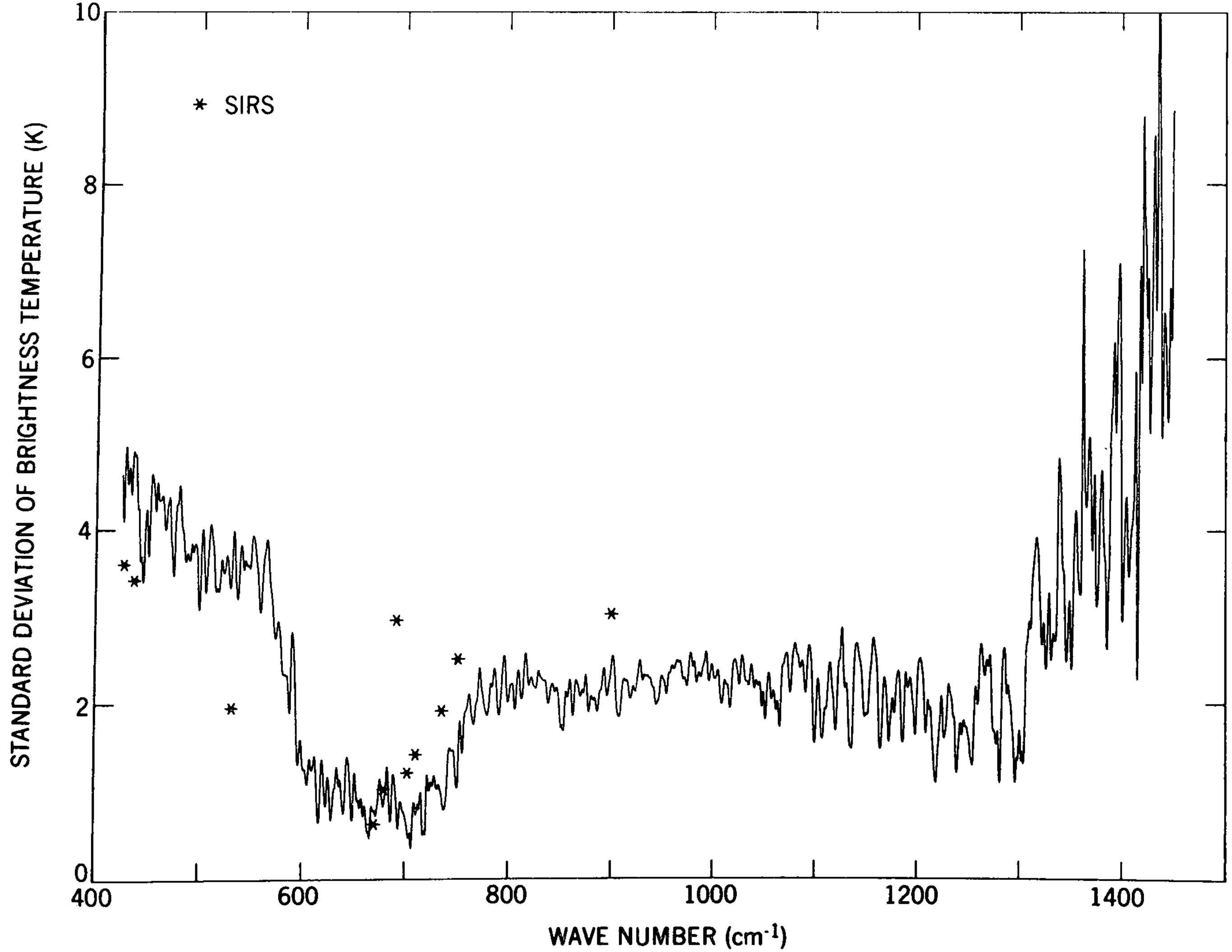

Figure 10. Standard deviation of brightness temperature corresponding to the average spectrum of Figure 9.

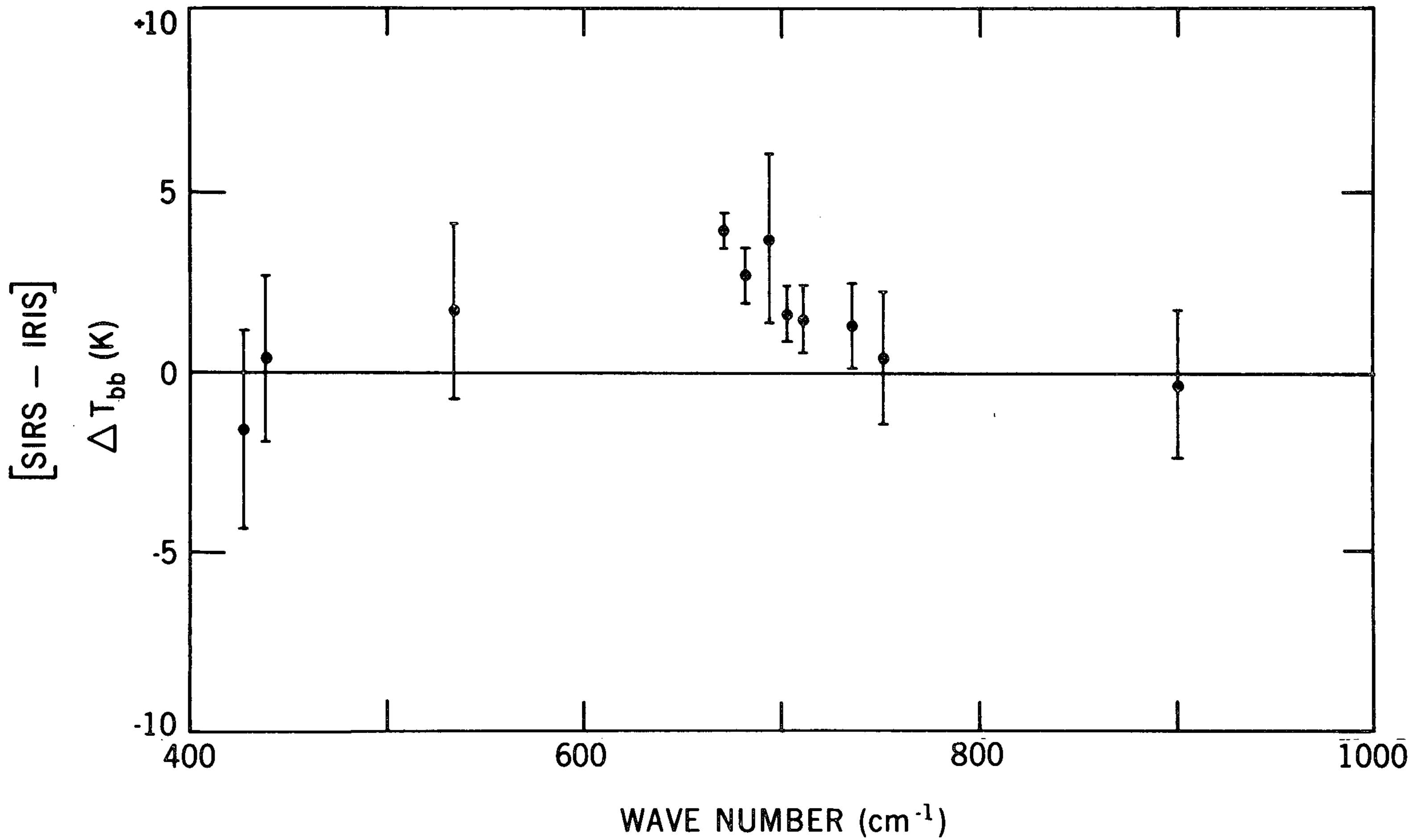

Figure 11. Average SIRS-IRIS difference for eight Wallops Island cases. The error bars are for one standard deviation.

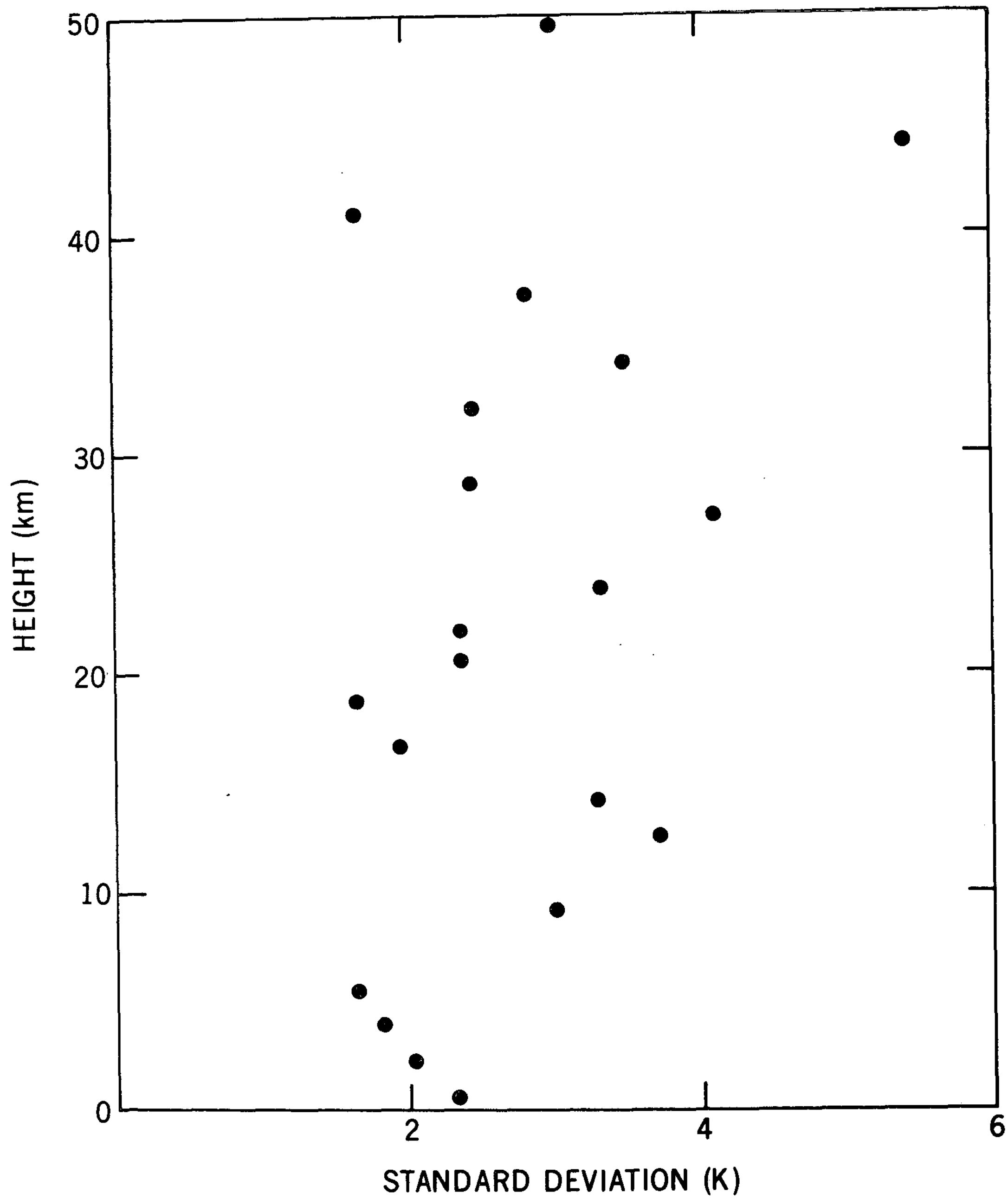

Figure 12. The standard deviation of the in-situ temperature measurements for the eight Wallops Island cases included in the average spectrum of Figure 9.

NASA–GSFC